Chinese Chemical Letters 37 (2026) 111633

Contents lists available at ScienceDirect

Chinese Chemical Letters

journal homepage: www.elsevier.com/locate/cclet

Achieving photo-controlled reversible multicolor luminescent supramolecular assembly by multicharged β-cyclodextrin

Rong Zhang[1], Zhiyi Yu[1], Hengyi Zhang, Yu Liu*

College of Chemistry, State Key Laboratory of Elemento-Organic Chemistry, Nankai University, Tianjin 300071, China

ARTICLE INFO

Article history:
Received 7 April 2025
Revised 7 July 2025
Accepted 23 July 2025
Available online 5 August 2025

Keywords:
Supramolecular assembly
Multicharged cyclodextrin
Multicolor luminescence
Photo-responsiveness
Dynamic anti-counterfeiting

ABSTRACT

Multivalent supramolecular assemblies not only can efficiently enhance the photophysical properties of functional molecules, but also are able to intelligently modulate the luminescence behavior. Herein, the photo-controlled reversible multicolor luminescent supramolecular assembly was constructed on agarose substrate by non-covalent interactions, which was composed of multicharged β-cyclodextrin (AMCD) with adamantane-modified spiropyrane derivative (Adam-SP) and tetraphenylethene derivatives (TPE). Firstly, the positively charged AMCD and negatively charged TPE form a binary assembly AMCD@TPE through electrostatic interaction, significantly enhancing the luminescence of TPE at 480 nm with a quantum yield (QY) jump from 0.68% to 31.24%. Moreover, the binary assembly AMCD@TPE and Adam-SP further formed a ternary assembly Adam-MC@AMCD@TPE through strong host-guest interaction, which not only achieved photo-regulated multicolor reversible fluorescence in both aqueous solution and agarose hydrogel under alternating visible light irradiation and dark treatment, but also produced adjustable luminescence changes under thermal stimulation. The ternary assembly Adam-MC@AMCD@TPE was successfully applied to photo-controlled multiple anti-counterfeiting.

Stimuli-responsive supramolecular luminescence system remains a research hotspot because it can widely apply in biological imaging [1,2], luminescent materials [3–6], and information anti-counterfeiting [7] through the response to various external stimuli such as temperature [8,9], light [10–12], electricity [13], polarity [14], force [15,16], humidity [17] and pH [18,19]. In particular, photo-responsive supramolecular luminescence systems based on molecular skeletons including diarylethylene [20], azobenzene [21], spiropyrane [22–25], and coumarin [26] have received extensive attention [27]. For example, Klajn and coworkers reported the photo-responsive nanoparticles in aqueous media by adsorbing hydrophobic thiolated azobenzene and water-soluble ligands terminated with the hydroxy group on the surface of Au nanoparticles, revealing the precisely regulated kinetic process of the isomerization of azobenzene by controlling the ratio of two ligands on the nanoparticles [28]. Wang group reported a light-controlled luminescent tunable supramolecular gel composed of di(benzylidene)-D-sorbitol, lanthanide ions ($Tb3^+$), diarylethylene (DTE), and spiropyran derivative (SP), which exhibited tunable fluorescence since the isomerization of DTE and SP could be regulated respectively under different wavelengths of UV and visible light irradiation, and was successfully applied to multiple information encryption [29]. Our group reported full-color lanthanide supramolecular photo-switch based on pillar[5]arene modified by 2,6-pyridinedicarboxylic acid (H), lanthanide ions (Ln^{3+}) and diarylethene modified by quaternary ammonium salt (G1). The non-covalent supramolecular assembly H/Ln^{3+}/G1 achieved multicolor fluorescence on/off by regulating the energy transfer between the photoinduced diarylethene isomers and the Ln^{3+} complex, which was used as a fluorescent ink for information encryption [30]. Although the photo-responsive supramolecular luminescence system has been developed [31,32], it is still a challenge to construct supramolecular assembly with bidirectional reversible multicolor luminescence. In the light-regulated supramolecular luminescence system, cyclodextrins, which possess various advantages such as excellent biocompatibility, low cost, and easy modification [33], are considered to be the ideal moiety for constructing supramolecular assemblies [34–38]. Herein, the photo-controlled reversible multicolor luminescent supramolecular hydrogel was constructed on agarose substrate by non-covalent interactions, which was composed of multicharged β-cyclodextrin (AMCD) with adamantane-modified spiropyrane derivative (Adam-SP) and tetraphenylethene derivatives (TPE). As shown in Scheme 1, firstly, the positively charged AMCD and negatively charged TPE form a binary assem-

* Corresponding author.
E-mail address: yuliu@nankai.edu.cn (Y. Liu).
[1] These authors contributed equally in this work.

https://doi.org/10.1016/j.cclet.2025.111633
1001-8417/

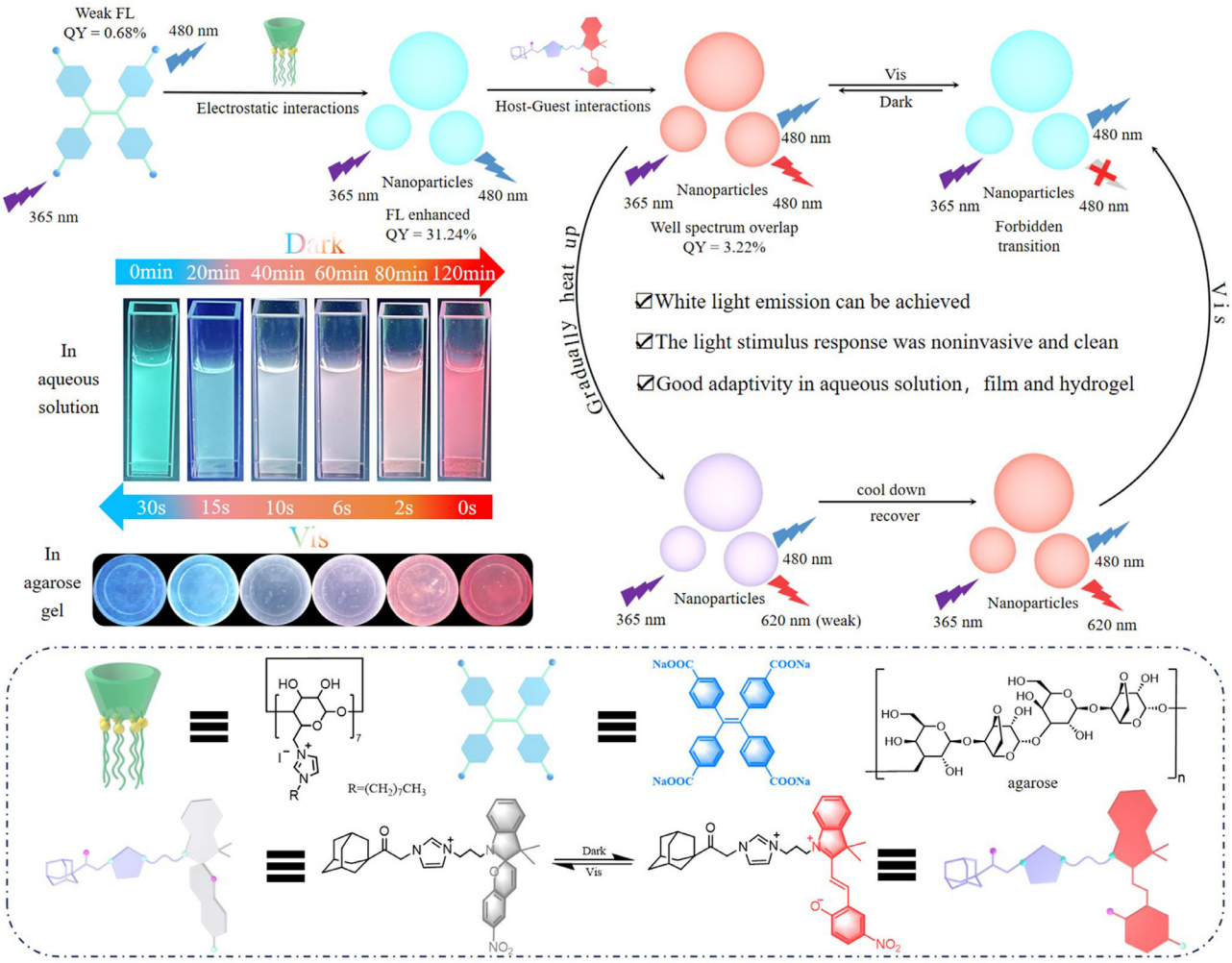

Scheme 1. Schematic of the multistage assembly and modulation of multicolor luminescence of AMCD, TPE, and Adam-SP.

bly AMCD@TPE through multivalent interactions to form nanoparticles, significantly enhancing the luminescence of TPE at 480 nm. Moreover, Adam-SP was further introduced into the system as a reversible photoswitch to construct a ternary assembly Adam-MC@AMCD@TPE through strong host-guest interaction, which not only achieved photo-regulated multicolor reversible fluorescence from blue to green, white, pink, orange, and red under alternating visible light irradiation and dark treatment, but also exhibited thermal responsive luminescence changes. The ternary assembly Adam-MC@AMCD@TPE was employed in photo-writing and self-erasing information encryption, which provided a new approach for constructing photo-modulated supramolecular luminescent assembly.

The amphiphilic cyclodextrin (AMCD) with polycationic features and hydrophobic alkyl chains, tetra-anionic tetraphenylethylene derivatives (TPE) was employed to construct the binary luminescent assembly. In addition, the adamantane-modified ring-closed spiropyran derivative, Adam-SP, was introduced into the supramolecular assembly to endow the system with photoswitching capabilities, which was synthesized through a substitution reaction between 1-(adamantan-1-yl)-2-(1*H*-imidazol-1-yl)ethan-1-one and 1′-(3-bromopropyl)-3′,3′-dimethyl-6-nitrospiro[chromene-2,2′-indoline] (Scheme S1 in Supporting information). The Adam-SP exhibited increased water solubility due to the presence of an imidazole group. The structure of Adam-SP and Adam-MC was characterized using nuclear magnetic resonance spectrometry (^{1}H NMR, ^{13}C NMR), and high-resolution mass spectrometry (HR-MS) (Figs. S1-S5 in Supporting information). First, the optical transmittance was initially evaluated to monitor the assembly of AMCD and TPE, as well as determine the optimal concentration for their successful assembly. In the presence of TPE monomer, there was a slight decrease in transmittance with an increase in concentration, specifically in the region above 450 nm where TPE itself did not exhibit absorption (Fig. S11 in Supporting information). After the introduction of AMCD into the system, a rapid decrease in optical transmittance was observed until the concentration of AMCD reached 9.1 μmol/L (Figs. 1a and b). Subsequent addition of AMCD led to an increase in transmittance, which can be attributed to the balanced presence of positive and negative charges at the critical aggregation concentration (CAC), further addition of positive charge disrupts the pre-existing assembly [33]. The test results demonstrate the weak self-aggregation phenomenon of TPE itself, no significant Tyndall phenomenon was observed (Fig. 1b, insert 1). Upon the addition of AMCD to the system, electrostatic interactions induce the self-aggregation phenomenon of TPE, resulting in a decrease in solution transmittance and an obvious Tyndall effect (Fig. 1b, insert 2), with a significant reduction in critical aggregation concentration value. Conversely, when maintaining a fixed concentration of AMCD, the optimal concentration of TPE can be achieved by employing TPE as back titration (Fig. S12 in Supporting information). In this case, the critical aggregation concentration is reached at an increased TPE concentration of 18.6 μmol/L and

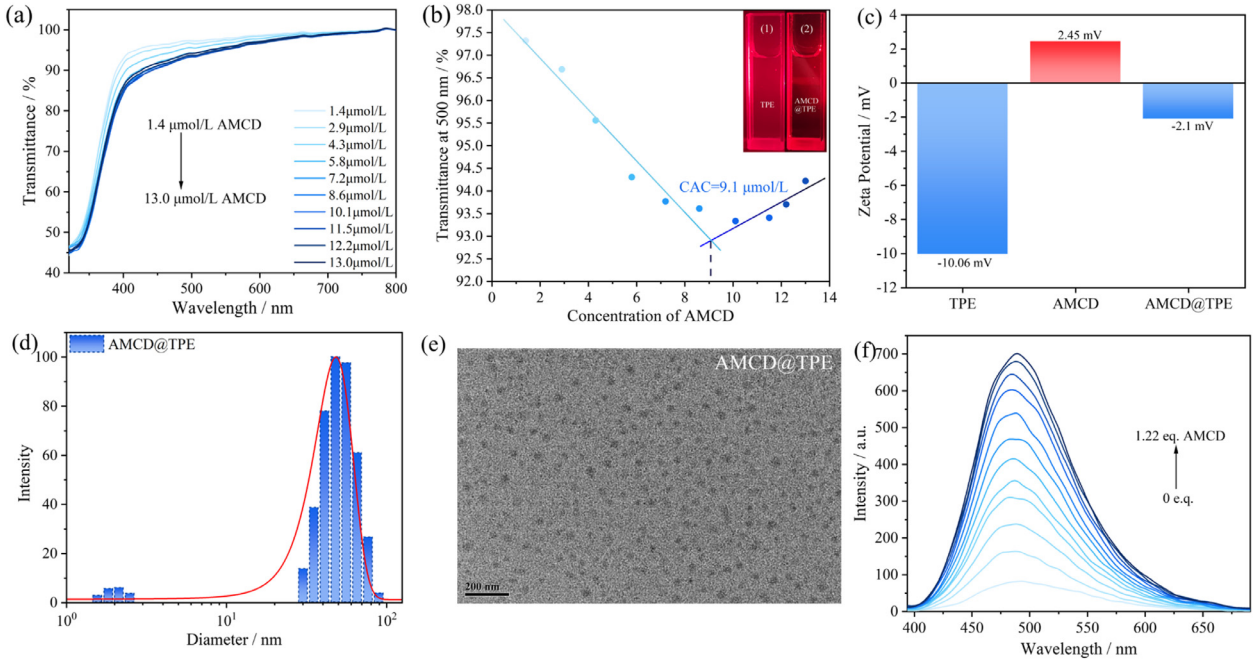

Fig. 1. (a) Fixed TPE concentration unchanged, optical transmittance test for AMCD@TPE ([TPE] = 20 μmol/L, 25 °C). (b) AMCD titrated TPE, transmittance change at 500 nm, [CAC] = 9.1 μmol/L. (c) The zeta potential gram of TPE, AMCD, and AMCD@TPE, 25 °C ([AMCD] = 2.4 μmol/L, [TPE] = 5 μmol/L). (d) DLS result of AMCD@TPE ([AMCD] = 2.4 μmol/L, [TPE] = 5 μmol/L). (e) TEM image of AMCD@TPE ([AMCD] = 2.4 μmol/L, [TPE] = 5 μmol/L). (f) Fluorescence titration of binary assembly AMCD@TPE ([TPE] = 15 μmol/L, [AMCD] = 0–316.6 μmol/L).

transmittance is reduced to 94.8 %. By comparing positive titration and inverse titration results, it is calculated that the optimal assembly effect is obtained when maintaining a concentration ratio of AMCD@TPE at 1:2.04. Subsequently, the concentrations of AMCD and TPE were adjusted to 7.2 and 15 μmol/L, respectively, based on the optimal ratio.

Next, the photoluminescence enhancement of the binary assembly induced by AMCD through electrostatic interactions was investigated. The fluorescence titration experiments indicated that the aqueous solution of TPE emitted an extremely weak fluorescence centered at 480 nm (Fig. S13 in Supporting information). Due to the aggregation-induced emission property of TPE, the luminescence intensity of AMCD@TPE enhanced with the increasing AMCD concentration until it reached a value of 1.22-fold equivalent, whereupon fluorescence enhancement peaked (Fig. 1f). The results demonstrated that poly-cationic cyclodextrin AMCD enhanced TPE's photoluminescence intensity to the original a dozen or so times through electrostatic interactions. The electrostatic assembly effect of the assembly was further investigated through the zeta potential experiment (Fig. 1c). At 25 °C, TPE exhibited an electric potential of −10.06 mV, AMCD had a potential of +2.45 mV, the small positive zeta potential of AMCD should be due to its low concentration (2.4 μmol/L). And the binary assembly showed a potential of −2.1 mV, possibly due to the distribution of negatively charged TPE around AMCD. Consequently, the resulting binary assembly nanoparticles can assemble with functional molecules through hydrophilic, hydrophobic interactions and electrostatic interactions. To investigate the basic morphology of AMCD@TPE, transmission electron microscopy (TEM) and dynamic light scattering (DLS) were employed. TEM images revealed that the particle size distribution of AMCD was uneven, ranging from 50–200 nm due to self-aggregation at the selected concentration which mainly depends on hydrophilic and hydrophobic interactions, while TPE and AMCD@TPE exhibited uniform nanoparticles with a size of approximately 20 nm (Fig. 1e and Fig. S14b in Supporting information), indicating successful assembly. DLS experiments showed that the effective diameters of AMCD, TPE, and AMCD@TPE were 685.30, 40.24, and 209.96 nm respectively (Fig. 1d and Fig. S15 in Supporting information), this is consistent with the results given by TEM.

In order to achieve photo-responsiveness of the supramolecular system, Adam-SP was introduced as an imperative component for further assembly with the binary assemblies AMCD@TPE through host-guest interactions. To confirm whether the spiropyran moiety contributed to the optical switching performance of Adam-SP, it was characterized using ^{1}H NMR (Fig. 2a). A small amount of DCl was added to DMSO for the ring-closed form better conversion to the ring-open form (Adam-MC). For testing purposes, Adam-MC form was irradiated under a UV lamp (365 nm) for 3 min before conducting tests in quick succession. It was observed that the protons in the spiropyran part of Adam-SP are shifted to the low field, which indicates that Adam-SP can be reversely converted to Adam-MC by placing it in darkness or subjecting it to UV radiation. Furthermore, the UV–vis absorption spectra of equal concentration gradients of Adam-MC were tested to establish an absorption intensity-concentration standard curve (Fig. S16 in Supporting information). According to the one-to-one relationship between the intensity of the Adam-SP's characteristic absorption peak at 515 nm and solution concentration, the photoisomerization extent of Adam-SP after one light-dark cycle could be obtained (Fig. 2b). Finally, based on measurements taken after keeping Adam-SP in darkness for 120 min (abs. = 0.241) and subjecting it to light for only 15 s followed by another period of darkness lasting for another 120 min (abs. = 0.179), we calculated that the conversion rate reached approximately 62.5 %. Moreover, the fluorescence spectra of Adam-SP with increasing temperature (Fig. S17 in Supporting information) shows that the fluorescence peak of Adam-SP at 620 nm decrease after heating, indicating that Adam-MC could undergo ring-close Adam-SP through thermal activation. To investigate the light responsiveness of Adam-SP upon the introduction of spiropyran, we examined its UV–vis absorption spectra under various light conditions (Fig. 2c). The results revealed that after 120 min in dark-

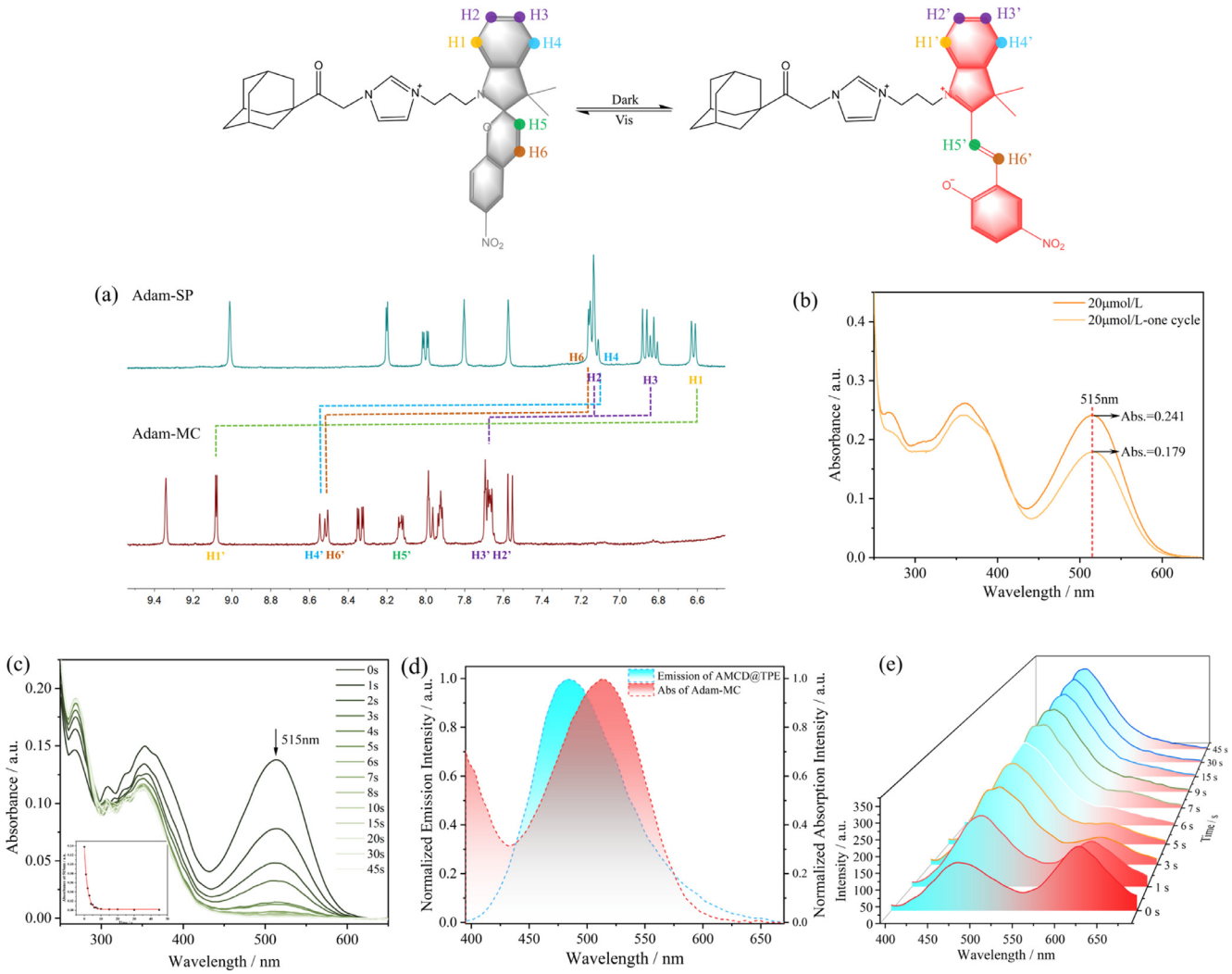

Fig. 2. (a) ^{1}H NMR spectrum of Adam-SP in DMSO–d_6, which was kept in light before testing; ^{1}H NMR spectra of Adam-MC in DMSO–d_6 ([DCl] = 20 mmol/L). (b) UV–vis absorption spectrum of Adam-MC after dark and one light-dark cycle, 25 °C. (c) UV–vis absorption spectrum of Adam-MC (20 μmol/L) during 0–30 s illumination, the solution was left in the dark for 120 min before testing (Insert: curve of absorption intensity at 515 nm as a function of illumination time). (d) UV–vis absorption spectrum of Adam-MC and emission spectrum of AMCD@TPE ([AMCD] = 7.2 μmol/L, [TPE] = 15 μmol/L, 25 °C). (e) Fluorescence emission spectrum of Adam-MC@AMCD@TPE ([Adam-MC] = 20 μmol/L, [AMCD] = 2.4 μmol/L, [TPE] = 5 μmol/L, 25 °C).

ness, the solution exhibited two distinctive absorption peaks at 360 nm and 515 nm. The absorption peak at 515 nm corresponds to Adam-MC in the ring-open state. Upon continuous irradiation with visible light, the intensity of the peak at 515 nm gradually diminished. After 30 s, it almost completely disappeared while an absorptive point emerged at 300 nm which confirms the occurrence of isomerization. This process can be reversed through thermal relaxation in darkness after a duration of 120 min. Furthermore, under cyclic stimulation alternating between dark and light conditions, reversible recovery of the absorption peak at 515 nm was observed in the UV–vis absorption spectra (Fig. S18 in Supporting information). The results demonstrated that the incorporation of spiropyran conferred a favorable light-responsive behavior upon the guest molecule.

In view of the retained assembly sites of the binary assemblies and the ability of the spiropyran moiety to generate the fluorescence switching in conjunction with photoisomerization, it was hypothesized to be able to achieve effective fluorescence resonance energy transfer (FRET) between AMCD@TPE and Adam-MC/SP. As depicted in Fig. 2d, the emission peak of AMCD@TPE binary assembly appears around 480 nm, while the absorption peak of ring-open Adam-MC occurs at 515 nm. The FRET could take place base on the substantial spectral overlap between the emission peak of AMCD@TPE and the absorption band of ring-open Adam-MC. Furthermore, due to electrostatic interactions between AMCD and TPE as well as host-guest interactions between β-cyclodextrin and adamantane, the distance between the two fluorophores decreases, facilitating FRET process. Subsequently, fluorescent titration was performed on AMCD@TPE binary assembly with various concentrations of Adam-MC to determine its optimal concentration in ternary assembly. As shown in Fig. 2e, when Adam-MC concentration reaches 20 μmol/L, both TPE (480 nm) and Adam-MC (620 nm) exhibit maximum emission peak intensities within ternary assembly. The titration test was also conducted for ring-closed Adam-SP, and the outcome demonstrated that the optimal luminous effect was still achieved at a concentration of 20 μmol/L (Fig. S19 in Supporting information). That's probably because when the concentration of Adam-MC is 20 μmol/L, it is hypothesised that the multiple weak interaction forces between Adam-MC and the AMCD@TPE balance each other and exhibit optimal co-assembly, resulting in

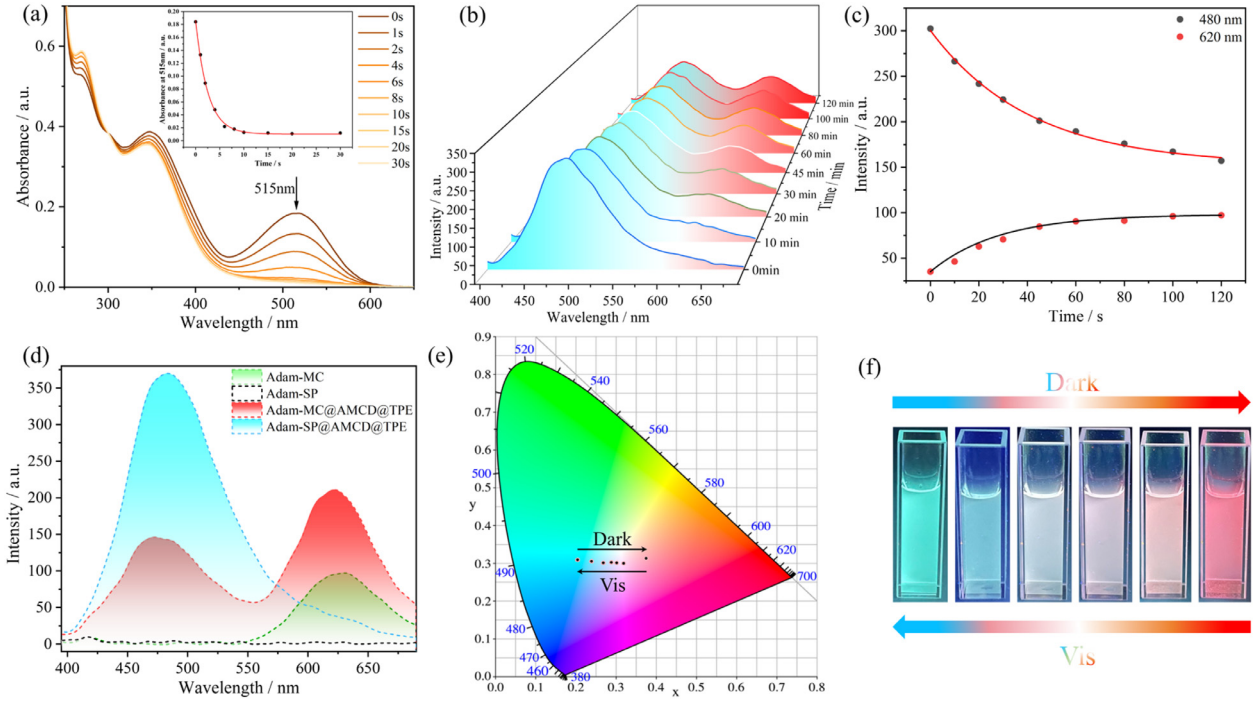

Fig. 3. (a) UV–vis absorption spectrum of Adam-MC@AMCD@TPE during 0–30 s illumination, the solution was left in the dark for 120 min before testing. Insert: curve of absorption intensity at 515 nm as a function of illumination time. (b) Changes in the fluorescence spectra of Adam-SP@AMCD@TPE in the dark. (c) Curve of emission intensity at 480 nm and 620 nm as a function of illumination time. (d) Fluorescence spectra of Adam-MC, Adam-SP, Adam-MC@AMCD@TPE and Adam-SP@AMCD@TPE (365 nm Ex for Adam-SP/Adam-MC, 520 nm Ex for ternary assembly). (e) 1931 CIE chromaticity diagram of Adam-MC@AMCD@TPE upon alternating visible irradiation and keeping in the dark. (f) The Adam-MC@AMCD@TPE solution undergoes a color change upon visible light irradiation and keep in the dark, as observed through photography. The concentrations used in the above experiments are [Adam-MC]=[Adam-SP] = 20 μmol/L, [AMCD] = 2.4 μmol/L, [TPE] = 5 μmol/L.

a more effective energy transfer efficiency and the maximum fluorescence intensity at 480 nm and 620 nm. Therefore, henceforth setting Adam-MC concentration at 20 μmol/L for subsequent tests.

Benefiting from the strong bonding ability between cyclodextrins and adamantane, the molecules with adamantane moiety and cyclodextrins were able to rapidly form supramolecular complexes in the aqueous phase. Due to the poor water solubility of AMCD, the assembly behavior was investigated by ^{1}H NMR titration using the reference molecules natural β-cyclodextrin and Adam-SP (Fig. S20 in Supporting information). Compared to the spectra containing only Adam-SP monomer, the addition of 2, 4, and 6 equiv. β-CD resulted in a downfield shift of the adamantane proton peak, indicating successful encapsulation of the adamantane moiety of Adam-SP into the β-CD cavity through host-guest interaction [39]. In order to investigate the photoresponseness of the ternary assembly Adam-SP@AMCD@TPE, the UV–vis absorption spectrum was examined (Fig. 3a). Similar to the binary assembly condition, the spectrum also exhibits an absorption peak attributed to spiropyran at 515 nm. The intensity of this peak gradually diminishes with increasing illumination time and reaches zero after approximately 30 s. During thermal relaxation in darkness, the intensity of the 515 nm absorption peak gradually recovers and stabilizes after a dark period of about 120 min (Fig. S21 in Supporting information). Moreover, to confirm that the fluorescence emission of the binary and ternary assemblies was independent of the excitation wavelength, fluorescence excitation mapping spectra were scanned for them (Fig. S22 in Supporting information). The binary assemblies exhibited stable blue fluorescence emission when the excitation wavelengths were varied in the range of 295–365 nm, and similarly, the ternary assemblies under dark conditions showed certain fluorescence emission centered at 480 nm and 620 nm varying with the excitation wavelengths from 280 nm to 375 nm. The experimental results demonstrated that changing the excitation wavelength only affects the intensity of the emission peak, but does not impact the emission wavelength, which suggests that the system does not possess excitation-dependent characteristics. The photoresponse photoluminescent behavior of the ternary supramolecular system was monitored using fluorescence spectra. The spectra revealed a gradual quenching of TPE emission at 480 nm with increasing darkness time, while the emission peak of Adam-MC at 620 nm gradually increased. It is shown that energy is gradually transferred from TPE to Adam-MC through the FRET process ($\Phi_{ET} = 47.73\,\%$) as the darkness time increases (Figs. 3b and c). Additionally, when the aqueous solution of Adam-MC@AMCD@TPE was exposed to visible light for 30 s, the fluorescence emission returned reversibly to its initial state (Fig. S23 in Supporting information). At the same time, it has good cycling stability, and the fluorescence intensity does not change significantly after 5 dark-light cycles (Fig. S24 in Supporting information). Additionally, we have observed successful excitation of the ternary assembly at 365 nm, whereas Adam-MC does not exhibit emission at this wavelength but can emit red fluorescence when excited at 520 nm. This suggests that through the synergism of electrostatic and host-guest interactions, the luminescent behavior of the assembly can be modulated (Fig. 3d and Table S1 in Supporting information). Not only that, the fluorescence emission process from blue to red and the visible light-induced inverse process can be observed by both the naked eye and camera when the solution is placed in darkness under 365 nm excitation (Fig. 3f). These observations are consistent with the results obtained from the 1931 CIE chroma diagram, which was utilized during thermal relaxation in darkness and visible light irradiation. The reversible transition from (0.1995, 0.3139) to (0.3748, 0.3128) can be achieved (Fig. 3e). Moreover, the fluorescence spectra confirmed that the luminescence behavior of the assembly in agarose hydrogel was similar as that in aqueous solution (Fig. S25 in Supporting information). In addi-

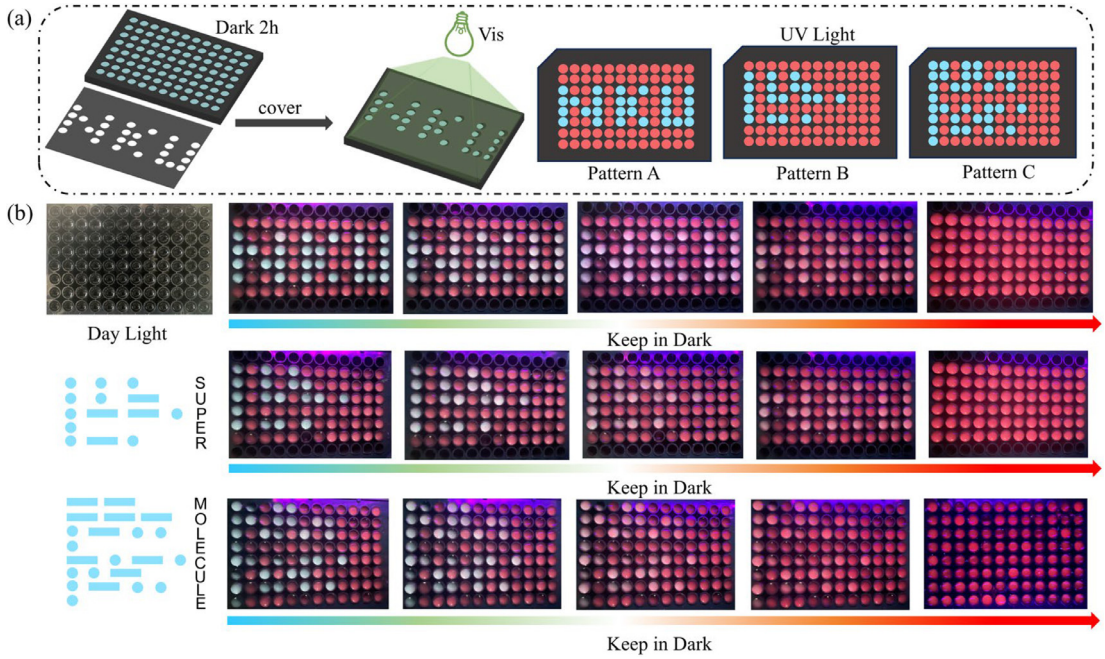

Fig. 4. (a) The Adam-SP@AMCD@TPE ternary supramolecular system enables information writing and erasing through visible light and dark stimuli. (b) The Morse code representing "super" and "molecule" was written under visible light, and the photo was read under ultraviolet light ([Adam-SP@AMCD@TPE] = 20 μmol/L, [AMCD] = 2.4 μmol/L, [TPE] = 5 μmol/L).

tion, transient fluorescence spectroscopy was employed to examine the lifetime of the binary assembly at 480 nm and the ternary assembly at 620 nm under different conditions (Fig. S26 in Supporting information). The results demonstrate that AMCD@TPE exhibits a lifetime of 5.18 ns, while Adam-SP@AMCD@TPE and Adam-MC@AMCD@TPE display lifetimes of 3.30 ns and 2.51 ns, respectively. The quantum yields for TPE and AMCD@TPE upon excitation at 365 nm are determined as 0.68 % and 31.24 %. Moreover, the quantum yield excited by Adam-MC at 520 nm is measured as 1.89 %, whereas that excited by Adam-MC@AMCD@TPE at 365 nm reaches up to 3.22 %. These findings indicate a significant enhancement in the luminescence behavior of guest molecules due to the synergistic effect between electrostatic interaction and host-guest interaction (Fig. S27 in Supporting information). Finally, DLS and TEM techniques were utilized to characterize the morphology of the ternary assembly, revealing minimal changes compared with both binary assembly (or free guest) before and after assembly; moreover, an effective diameter of approximately 209.96 nm was obtained through DLS measurements (Fig. S28 in Supporting information). In addition, the ternary assembly is also highly responsive to temperature. As shown in Fig. S29 (Supporting information), with the increase in temperature, the emission peak intensity of Adam-MC@AMCD@TPE at 480 nm and 620 nm will gradually decrease, but the red emission at 620 nm will decrease more strongly, in 1931 CIE chromaticity diagram, we can see that the color of the assembly will switch between lavender and red with the heating and cooling process. This may be due to the fact that adamantane falls out of the cavity of cyclodextrin with increasing temperature leading to unassembly [40,41]. At this time, the distance between TPE and Adam-MC is too far, resulting in a decrease in the efficiency of the energy transfer process. Moreover, the assembly showed only slight fatigue after five cycles, indicating that Adam-MC@AMCD@TPE has a good response to temperature and cycle reversibility.

Different from conventional photoresponsive security systems, the Adam-SP@AMCD@TPE supramolecular system enables bidirectional reversible dynamic information encryption. This is achieved through its ability to respond to reversible light-induced isomerization, resulting in the formation of fluorescence patterns with distinct colors during the process of information writing and interpretation (Fig. 4a). The Adam-SP@AMCD@TPE solution was uniformly dispensed into a 96-well plate and kept in darkness for 120 min. Subsequently, a self-made black hollow cardboard with an "NKU" pattern (abbreviation of Nankai University) was placed on top of the plate, which was then irradiated for 30 s using a visible lamp emitting light at a wavelength of 530 nm. Upon observation under daylight conditions, no discernible information was visible initially. However, when exposed to a 365 nm UV lamp, it became apparent that the region previously illuminated by the visible lamp displayed the word "NKU" in blue while the unexposed area appeared red. Over time, as the solution remained either in darkness or under continuous UV irradiation, the color sequence of "NKU" transitioned from blue to green, white, orange, and finally to red. At this stage, interpretation under ultraviolet light at 365 nm became impossible due to erasure caused by dark or UV stimulation. Furthermore, leveraging this system's reversible characteristics under cyclic dark-light stimulation allows for the sequential generation and erasure of various patterns through light-induced writing followed by erasure *via* dark or ultraviolet irradiation. As depicted in Fig. 4b, Morse code representing "super" is written upon exposure to visible light; its color changes over time spent in darkness until eventual erasure occurs within this environment; subsequently replaced by Morse code representing "molecule," which undergoes similar erasure once again within darkness.

It is worth noting that, in addition to writing and erasing information in solution, the supramolecular assembly also exhibited excellent photochromic properties when incorporated into PVA films. To prepare the film, 0.5 g of PVA was added to 5 mL of secondary water and stirred at 95 °C for 2 h until complete dissolution. The mixture was then cooled to room temperature before adding Adam-SP@AMCD@TPE. The resulting solution was poured onto a slide and subjected to oven treatment for 1 h until film formation occurred. Under sunlight, the prepared PVA film appears colorless and transparent; however, after being irradiated by

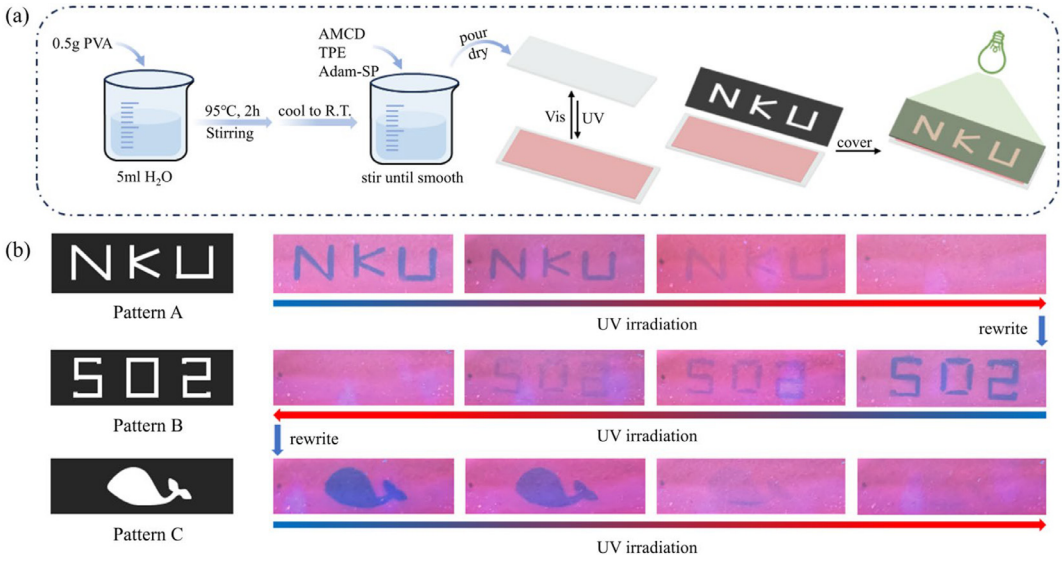

Fig. 5. (a) The Adam-SP@AMCD@TPE ternary supramolecular system enables information writing and erasing through visible light and UV stimuli in PVA film. (b) The "502" and whale pattern was written under visible light, and the photo was read under ultraviolet light.

an ultraviolet lamp for 30 s, it turns red. Remarkably, upon exposure to visible light from a lamp source, the film can be restored back to its original transparent and colorless state, indicating that Adam-SP@AMCD@TPE not only demonstrates excellent reversible light responsiveness in solution but also on solid substrates such as this PVA film. The self-erasure performance of the Adam-SP@AMCD@TPE-PVA film is illustrated in Fig. 5. In order to observe this phenomenon, the film was covered with a self-made black hollow cardboard featuring the word "NKU". Information was written onto the film using visible light while erasing was achieved through irradiation with an ultraviolet lamp. This process involved repeated writing and erasing cycles using both "502" text and a whale pattern - during which time the photoresponsive nature of the film remained intact for continued use.

In summary, photo-controlled reversible multicolor luminescent supramolecular assembly was constructed through supramolecular cascade assembly, which mainly depends on multivalent interactions between multi-charged amphiphilic AMCD and negatively charged TPE and strong host-guest interactions of AMCD encapsulating Adam-SP in agarose substrate. Taking advantage of the photoisomerization of Adam-SP, the multivalent supramolecular assembly Adam-SP@AMCD@TPE not only achieved photo-controlled multicolor reversible luminescence from blue to red through an effective FRET process upon alternating visible light irradiation and darkness, but also modulated luminescence changes in response to thermal stimuli. Due to the tunable luminescence properties of this ternary supramolecular system, it has been successfully applied to dynamic information encryption. This work provided a novel approach for constructing intelligent luminescent supramolecular assembly through cascade assembly.

Declaration of competing interest

The authors report no declarations of interest.

CRediT authorship contribution statement

Rong Zhang: Writing – original draft, Investigation. **Zhiyi Yu:** Methodology. **Hengyi Zhang:** Methodology. **Yu Liu:** Writing – review & editing, Funding acquisition.

Acknowledgments

We thank National Natural Science Foundation of China (NSFC, Nos. 22131008 and 22271165), Natural Science Foundation of Tianjin (No. 22JCYBJC00500) and the Haihe Laboratory of Sustainable Chemical Transformations for financial support.

Supplementary materials

Supplementary material associated with this article can be found, in the online version, at doi:10.1016/j.cclet.2025.111633.

References

[1] H.J. Wang, W.W. Xing, Z.H. Yu, et al., Chin. Chem. Lett. 35 (2024) 109183.
[2] X.L. Hu, H.Q. Gan, W.Z. Gui, et al., Proc. Natl. Acad. Sci. U. S. A. 121 (2024) e2408716121.
[3] W.W. Xu, Y. Chen, X. Xu, Y. Liu, Small 20 (2024) 2311087.
[4] Q. Li, H. Zhang, K. Lou, et al., Proc. Natl. Acad. Sci. U. S. A. 119 (2022) e2121746119.
[5] Y.D. Yang, X. Ji, Z.H. Lu, et al., Nat. Commun. 11 (2020) 77.
[6] Y. Shen, X. Le, Y. Wu, T. Chen, Chem. Soc. Rev. 53 (2024) 606–623.
[7] Y. Tian, B. Huang, S. He, et al., Adv. Funct. Mater. 34 (2024) 2419865.
[8] M. Su, Y. Song, Chem. Rev. 122 (2022) 5144–5164.
[9] B. Saha, B. Ruidas, S. Mete, et al., Chem. Sci. 11 (2020) 141–147.
[10] H. Wang, H. Xing, J. Gong, et al., Mater. Horiz. 7 (2020) 1566–1572.
[11] X.M. Cai, S. Li, W.J. Wang, et al., Adv. Sci. 11 (2024) 2307078.
[12] Y. Yao, S. Chen, C. Yan, et al., Angew. Chem. Int. Ed. 64 (2025) e202416963.
[13] S.L. Li, M. Han, Y. Zhang, et al., J. Am. Chem. Soc. 141 (2019) 12663–12672.
[14] J. Zhang, A. Li, H. Zou, et al., Mater. Horiz. 7 (2020) 135–142.
[15] G. Huang, Y. Jiang, S. Yang, B.S. Li, B.Z. Tang, Adv. Funct. Mater. 29 (2019) 1900516.
[16] Y. Zhang, Y. Chen, J.Q. Li, S.E. Liu, Y. Liu, Adv. Sci. 11 (2024) 2307777.
[17] M. Yang, S.Q. Wang, Z. Liu, et al., J. Am. Chem. Soc. 143 (2021) 7732–7739.
[18] N. Majcen, R. Mohsen, M.J. Snowden, J.C. Mitchell, B. Voncina, Adv. Colloid Interface Sci. 256 (2018) 193–202.
[19] T. Dünnebacke, N. Niemeyer, S. Baumert, et al., Nat. Commun. 15 (2024) 5695.
[20] Y. Zhang, C. Zhang, Y. Chen, et al., Adv. Opt. Mater. 10 (2022) 2102169.
[21] Y. He, Z.Y. Zhang, M. Xie, C. Yu, T. Li, Angew. Chem. Int. Ed. 60 (2021) 16539–16546.
[22] A. Meeks, M.M. Lerch, T.B.H. Schroeder, A. Shastri, J. Aizenberg, J. Am. Chem. Soc. 144 (2022) 219–227.
[23] H. Zhang, Y. Zhang, Y. Chen, et al., Eur. Polym. J. 192 (2023) 112070.
[24] X. Yang, M. Du, Z. Chu, C. Li, Adv. Mater. 37 (2025) 2500857.
[25] X. Chen, X.F. Hou, X.M. Chen, Q. Li, Nat. Commun. 15 (2024) 5401.
[26] G. Wang, X. Huang, Z. Zhou, Y. Zhang, Y. Yu, Chem. Eng. J. 499 (2024) 155820.
[27] X. Wang, B. Xu, W. Tian, Acc. Mater. Res. 4 (2023) 311–322.
[28] Z. Chu, Y. Han, T. Bian, et al., J. Am. Chem. Soc. 141 (2019) 1949–1960.
[29] X. Cong, K. Ou, J. Ma, et al., Chem. Eng. J. 481 (2024) 148355.

[30] W.L. Zhou, X.Y. Dai, W. Lin, Y. Chen, Y. Liu, Chem. Sci. 14 (2023) 6457–6466.
[31] R. Zhang, Y. Chen, Y. Liu, Angew. Chem. Int. Ed. 62 (2023) e202315749.
[32] Y. Tian, B.T. Huang, S. He, et al., Angew. Chem. Int. Ed. 35 (2024) 2419865.
[33] Z.X. Liu, Y. Liu, Chem. Soc. Rev. 51 (2022) 4786–4827.
[34] Z. Liu, H. Chen, M. Tian, et al., Aggregate 5 (2024) e627.
[35] G. Crini, S. Fourmentin, É. Fenyvesi, et al., Environ. Chem. Lett. 16 (2018) 1361–1375.
[36] H.M. Yu, X.Y. Yu, Y. Chen, Y. Liu, Soft. Matter. 19 (2023) 3162–3166.
[37] G. Decool, M. Kfoury, L. Paitel, A. Sardo, S. Fourmentin, Environ. Chem. Lett. 22 (2024) 321–353.
[38] T. Kakuta, Y. Takashima, M. Nakahata, et al., Adv. Mater. 25 (2013) 2849–2853.
[39] K. Jackowski, M. Wilczek, Molecules 29 (2024) 2617.
[40] S. Rasouli, S.M. Hashemianzadeh, J. Mol. Liq. 390 (2023) 123096.
[41] X.L. Zhou, X. Zhao, X. Bai, Q.W. Cheng, Y. Liu, Adv. Funct. Mater. 34 (2024) 2400898.